Journal of Archaeological Science 101 (2019) 63–71

Contents lists available at ScienceDirect

Journal of Archaeological Science

journal homepage: www.elsevier.com/locate/jas

Spatiotemporal dynamics of prehistoric human population growth: Radiocarbon 'dates as data' and population ecology models

Erick Robinson[a,*], H. Jabran Zahid[b], Brian F. Codding[c], Randall Haas[d], Robert L. Kelly[a]

[a] Department of Anthropology, University of Wyoming, 1000 E. University Ave., Laramie, WY, 82071, USA
[b] Smithsonian Astrophysical Observatory, Harvard-Smithsonian Center for Astrophysics, 60 Garden St., Cambridge, MA, 02138, USA
[c] Department of Anthropology, University of Utah, 270 S. 1400 E., Salt Lake City, UT, 84112, USA
[d] Department of Anthropology, University of California, Davis, 1 Shields Ave., Davis, CA, 95616, USA

ARTICLE INFO

Keywords:
Radiocarbon dates
Time-series analysis
Spatial analysis
Population ecology
Ideal free distribution
Allee effects
Wyoming

ABSTRACT

Archaeologists now routinely use summed radiocarbon dates as a measure of past population size, yet few have coupled these measures to theoretical expectations about social organization. To help move the 'dates as data' approach from description to explanation, this paper proposes a new integrative theory and method for quantitative analyses of radiocarbon summed probability distributions (SPDs) in space. We present this new approach to 'SPDs in space' with a case study of 3571 geo-referenced radiocarbon dates from Wyoming, USA. We develop a SPD for the Holocene in Wyoming, then analyze the spatial distribution of the SPD as a function of time using a standard nearest-neighbor statistic. We compare population growth and decline throughout the Holocene with expectations for different Ideal Distribution Models from population ecology that predict the relationship between habitat quality and population density. Results suggest that populations in Wyoming were initially clustered and then became increasingly dispersed through the course of the Holocene. These results suggest that Allee-like benefits to aggregation, rather than ideal free-driven dispersion patterns, explain settlement decisions in response to growing populations. Our approach is a first step in constructing a method and theory for describing relationships between social organization and population growth trends derived from archaeological radiocarbon time-series.

1. Introduction

Statistical analyses of large radiocarbon datasets are a powerful approach to investigate prehistoric population growth in different regions of the world (Shennan and Edinborough, 2007; Peros et al., 2010; Kelly et al., 2013; Shennan et al., 2013; Timpson et al., 2014; Wang et al., 2014; Chaput et al., 2015; Tallavaara et al., 2015; Williams et al., 2015a; Chaput and Gajewski, 2016; Crema et al., 2016; Goldberg et al., 2016; Perez et al., 2016; Zahid et al., 2016). Critical appraisals of these analyses have focused on various external biases to establish the technique of using the summed probability distribution (SPD) of a set of radiocarbon dates as a population proxy (Surovell and Brantingham, 2007; Armit et al., 2013; Bamforth and Grund, 2012; Williams, 2012; Contreras and Meadows, 2014; Brown, 2015; Torfing, 2015; Freeman et al., 2017). Taphonomic bias (Surovell et al., 2009; Peros et al., 2010; Williams, 2012; Bluhm and Surovell, 2018), discovery bias (Williams, 2012; Shennan et al., 2013; Rhode et al., 2014; Timpson et al., 2014; Crema et al., 2017), and calibration bias (Shennan et al., 2013; Timpson et al., 2014; Brown, 2015; Carleton et al., 2018) have been examined. Treatment of these biases and comparisons with independent proxies of prehistoric population growth (e.g., Downey et al., 2014; Chaput and Gajewski, 2016; Zahid et al., 2016) have transformed the 'dates as data' approach (Rick, 1987) into a robust method for paleodemographic research.

Developing a theoretical framework for using statistical analyses of radiocarbon data to help understand human behavior and cultural evolution remains challenging. Fluctuations in SPDs are interpreted as changes in population size but may also be sensitive to changes in social organization (Crombé and Robinson, 2014; Naudinot et al., 2014) and energy consumption (Freeman et al., 2018). Thus, SPDs may provide a means to study social and ecological processes affecting prehistoric human populations. We demonstrate the use of radiocarbon data for understanding prehistoric population dynamics by performing a spatiotemporal analysis of the radiocarbon record to measure the spatial distribution of Holocene populations in Wyoming as a function of time.

Our analysis of the spatial distribution of the prehistoric population

* Corresponding author.
E-mail address: Erick.Robinson@uwyo.edu (E. Robinson).

https://doi.org/10.1016/j.jas.2018.11.006
Received 30 May 2018; Received in revised form 31 October 2018; Accepted 19 November 2018

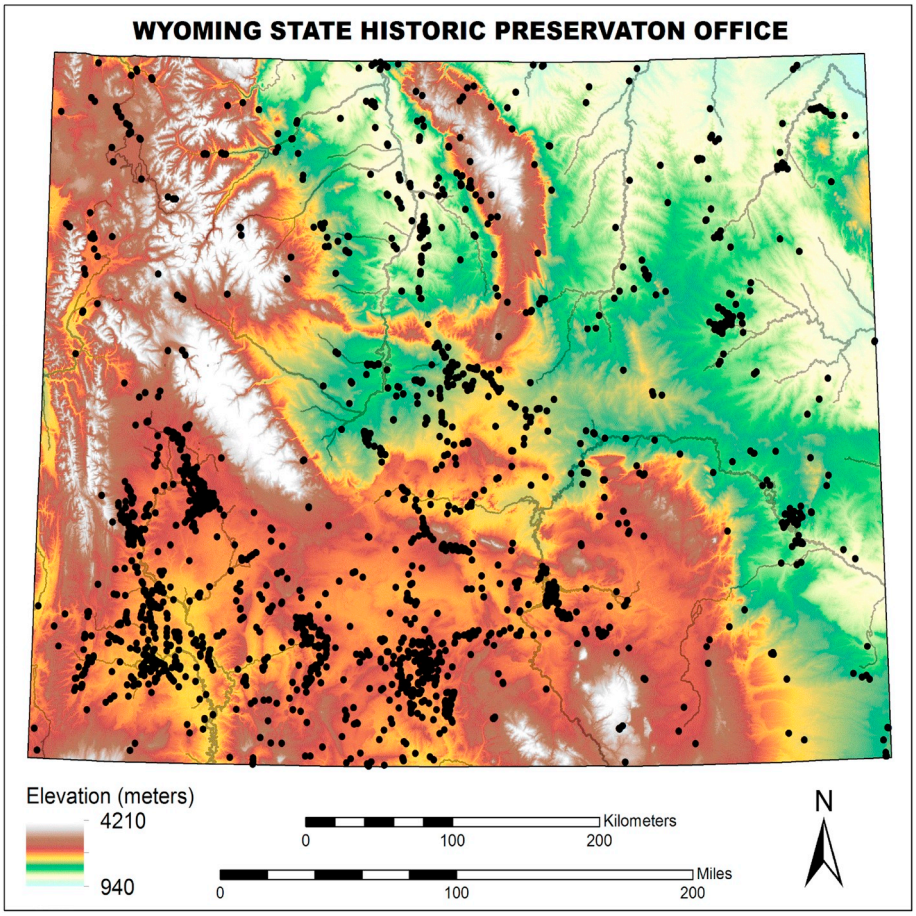

Fig. 1. Locations of all archaeological radiocarbon dates in the state of Wyoming (n = 4576), plotted on a digital elevation model. Courtesy of R. Hillman, Wyoming SHPO.

of Wyoming is motivated by recent results from Zahid et al. (2016). These authors measure the long-term population growth rate of foragers dwelling in Wyoming and Colorado during the early-middle Holocene, showing that this long-term growth rate is comparable to contemporaneous populations in continental Europe, North America and Australia; in continental Europe the population had transitioned to agriculture. The comparable long-term growth rates measured worldwide indicate that global climate or factors intrinsic to the species regulated the growth of human populations during much of the Holocene (Zahid et al., 2016). Bettinger (2016) suggests that one such factor may be human specific behavior patterns governing spatial organization. He proposes that the results of Zahid et al. (2016) may be interpreted within the framework of the Ideal Free Distribution (IFD) (Fretwell and Lucas, 1969) model from population ecology.

The IFD model describes the relationship between habitat selection, habitat suitability, and population growth in terms of negative density dependence. The first individuals in an area occupy the most suitable habitats, but as habitat suitability declines with population growth, individuals bud off and populate less productive unoccupied habitats. The population growth rate of 0.03–0.05% reported by Zahid et al. (2016) for both foragers and farmers worldwide during much of the early-middle Holocene might reflect limits on how fast a regional carrying capacity equilibrium "can be reached through the reshuffling of population between environments without disrupting social ties" (Bettinger, 2016, 814). Here we test this hypothesis by examining the spatial distribution of the prehistoric population of Wyoming inferred from the radiocarbon record.

Radiocarbon data have been analyzed using various geospatial statistical methods (Crema et al., 2010, 2017; Onkamo et al., 2012; Bevan et al., 2013; Williams et al., 2013, 2015a; Chaput et al., 2015; Park et al., 2017). These types of analyses may provide a means to investigate the impact of diachronic changes in social organization and land use on the production of radiocarbon time-series (Crombé and Robinson, 2014; Naudinot et al., 2014). In other words, the spatial distribution of the radiocarbon record may reflect patterns of social organization and thus provide a means to discriminate between various ecological models describing the spatial distribution of species.

Here we compare a spatiotemporal analysis of the radiocarbon record of Wyoming with the expected temporal evolution of a simple, nearest-neighbor statistic for various Ideal Distribution Models (IDMs). The use of formal theory from population ecology enables predictions for different kinds of spatial dynamics and their implication for prehistoric human population change. We propose that this approach of analyzing "SPDs in space" provides a means for understanding prehistoric transitions to competitive territorial systems and cooperative economies of scale.

2. Data and methods

Our parent sample is comprised of ca. 4715 radiocarbon dates from the state of Wyoming, acquired mostly from grey-literature cultural resource management reports and accessed via the WYCRO online database of the Wyoming State Historic Preservation Office Wyoming Cultural Resource Information System. Each radiocarbon date has its own point provenience, which is necessary for the spatial analysis. Spatial distribution of the radiocarbon dates is shown in Fig. 1. We correct for oversampling bias by combining multiple uncalibrated dates from the same site with differences <100 years by taking the error-

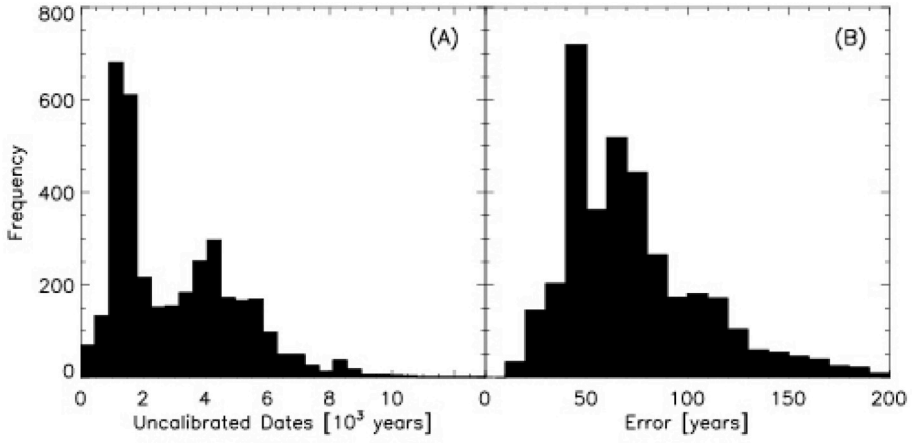

Fig. 2. Histogram of (A) uncalibrated dates analyzed in this work and (B) their corresponding errors.

weighted averaged in a pairwise manner starting with the smallest difference first. We remove dates with uncertainties >200 years as they are susceptible to systematic errors (Williams, 2012). This selection criteria yields 3571 dates for our analysis. Fig. 2 shows the distribution of uncalibrated dates and errors.

We calculate the SPD of the radiocarbon data by calibrating each date using the IntCal13 radiocarbon age calibration curve (Reimer et al., 2013). The error in each ^{14}C measurement is translated into a probability distribution of calibrated dates. We sum the probability distribution of the 3571 individual dates to produce the SPD. Each date is equally weighted in the sum.

The uncertainties in the SPD are determined from bootstrapping the data and account for observational, sampling and calibration uncertainties. We randomly sample, with replacement, 3571 dates from our analyzed sample to produce an SPD. We do this 10,000 times to derive the distribution's 68 and 95% confidence intervals.

We apply the taphonomic correction derived by Surovell et al. (2009):

$$N(t) = 5.726442 \times 10^{6}(t + 2176.4)^{-1.3925309}. \quad (1)$$

Here $N(t)$ is assumed to be constant and declines as a function of time t, given in units of calibrated years before present, due to taphonomic loss. Thus, we correct the SPD at each calibrated year by dividing by $N(t)$. We apply this correction only to consistently compare the growth rate we measure from the data with results from Zahid et al. (2016). The spatial analysis is completely independent of the taphonomic correction, as the taphonomic correction only affects the magnitude of the SPD, not the spatial coordinates of individual points.

We perform a clustering analysis by calculating the Clark-Evans (Clark and Evans, 1954) nearest neighbor statistic (NNS), R. The statistic is calculated by measuring the mean of the distance of each point in the sample to its nearest neighbor and comparing against the expectation for a randomly distributed sample population. Clark and Evans (1954) show that for a random distribution, the NNS value is equal to $1/(2\sqrt{\rho})$ where ρ is the population density. An $R = 1$ value corresponds to a random spatial distribution. Values <1 and >1 correspond to clustered and dispersed spatial distributions, respectively. The method of Clark and Evans (1954) is often applied in ecology where the spatial distribution of a sample is measured over a grid of fixed area and thus the density of the population, ρ, is straightforward to calculate (Perry et al., 2006; Velázquez et al., 2016).

A standard Clark-Evans analysis is not possible in this study because the data come from heterogeneous sources and thus the survey boundary is not well defined. We analyze radiocarbon dates within the modern borders of Wyoming but only a small fraction of the state has been surveyed for radiocarbon data. Without an accurate estimate of the survey area, we are unable to estimate the population density and thus can not analytically calculate the R value for a randomly distributed population to compare against. In this analysis, we empirically derive the random distribution. We note that while edge effects pose problems for second-order spatial point pattern analyses such as k-means clustering, first-order nearest neighbor statistics are less sensitive (Velázquez et al., 2016).

We apply a modified Clark-Evans nearest neighbor statistic calculated using code we developed in the programming language *IDL*. The modified statistic uses the empirical distribution of the data to derive the null hypothesis of the random distribution. We calculate NNS for the data as $\bar{r}_A = \sum r_i/N$ where r_i is the distance to nearest neighbor for radiocarbon date i; i goes from 1 to N where N is the number of dates in the sample.

To derive the null hypothesis, we assign a new spatial coordinate to each radiocarbon date by randomly drawing from the spatial distribution of all radiocarbon dates in the sample. Thus, the data set from which we derive the null hypothesis is composed of the same radiocarbon dates, but a new spatial coordinate which is randomly taken from the full distribution of spatial coordinates. In other words, we shuffle the spatial coordinates associated with each radiocarbon date by randomly drawing from the distribution of spatial coordinates in the sample. This procedure assumes that spatial distribution of the radiocarbon data is uncorrelated across the large timespan we analyze. We calculate the NNS of the randomly shuffled data in the same way as before; $\bar{r}_E = \sum r_j/N$ where j now goes from 1 to N. The Clark-Evans $R = \bar{r}_A/\bar{r}_E$.

We calculate R in bins of 500 years. Due to observational and calibration uncertainties, a measured $_{14}C$ date corresponds to a probability distribution of calibrated dates. We adopt the most probable date for each data point in our sample when binning the data. We perform the calculation in 50 year steps, thus there is a 450 year overlap between adjacent bins. When randomly shuffling the spatial coordinates, we shuffle the whole data set prior to binning. This approach explicitly assumes that the spatial coordinates are uncorrelated across the data set, thus random reshuffling of the spatial coordinates provides a means to calculate $\bar{r}_E$. We calculate uncertainties by bootstrapping; i.e., we calculate R 10,000 times with a different random shuffle when calculating $\bar{r}_E$.

We caution against over-interpreting the absolute R values, which we expect to be generally clustered independent of internal social dynamics due to the basic clustering effects of physiography and habitat constraints. As the digital elevation model in Fig. 1 shows, the topographic variability of Wyoming might generate biases for clustering in more lowland locations. However, as Fig. 1 highlights, the majority of our data comes from lowland locations, which means we have less potential for biases than if we had larger amounts of data points from upland mountainous locations. Despite cautioning against over-

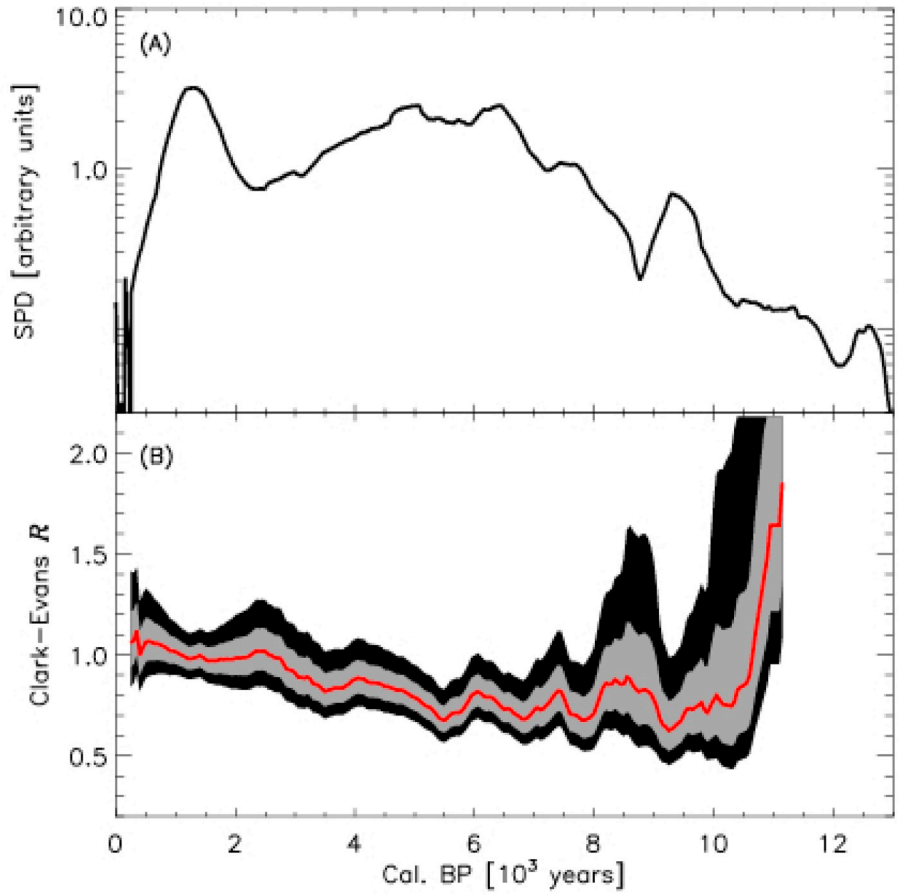

Fig. 3. (A) Summed probability distribution of the radiocarbon record for Wyoming plotted as a function of cal. BP. for the last 13,000 years. (B) Clark-Evans *R* calculated in bins of 500 years stepped by 50 years over 11,000 years. Red line is the mean of 10,000 realizations with grey and black representing the 68% and 95% confidence intervals, respectively. We do not display the *R* value before 11,000 Cal BP because the small sample size and large uncertainties. We boxcar smooth the results in (A) and (B) by 500 years. (For interpretation of the references to colour in this figure legend, the reader is referred to the Web version of this article.)

interpretation of the absolute R values, we do consider relative changes in the *R* value to be robust. Thus, directional trends may be interpreted within the framework we present.

3. Results: the size and spatial distribution of the prehistoric population

Fig. 3A shows the SPD for the data set over the past 13,000 years. For the period between 13000 and 6000 cal BP, the Wyoming radiocarbon record shows long term exponential growth as indicated by linear growth in the SPD when plotted on a log-linear scale. This long-term trend is similar to results reported in Zahid et al. (2016) and is expected since the data analyzed in this study significantly overlaps with the Zahid et al. (2016) sample.

We measure a long-term growth rate of 0.031 ± 0.012% for the population of Wyoming between 13000 and 6000 cal BP by fitting a linear model to the logarithm of the SPD as a function of time. The error bars are bootstrapped. This long-term rate of growth is consistent (~ 1σ) with the rate reported in Zahid et al. (2016) for Wyoming and Colorado over the same period. This growth rate corresponds to a doubling of the population every ~ 2000 years. From 6000 to 2000 cal BP the SPD shows a flattening followed by a decline. This is followed by a rapid increase in the SPD around ~ 2000 cal BP and a rapid decline starting ~ 1300 cal BP.

R values for the past 11000 years in Wyoming are plotted in Fig. 3B. The results indicate statistically robust deviations from random distributions (R = 1). The first-order trend from 11000 to 9000 cal BP is one of increasing clustering. From 9000 to 8000 cal BP there is a brief trend back to more dispersed distributions. This brief period of increased dispersions coincided with the first major climate change event during the Holocene (Shuman and Marsicek, 2016), with massive droughts in lowland regions leading to greater focus on upland settlements in richer and more diverse ecosystems (Kelly et al., 2013). At 8000 cal BP there is a clear directional change in the first-order trend of *R* values. From 8000 cal BP to present there is an overall increase towards a dispersed distribution. Interestingly, despite this overall increase towards more dispersed distributions, the period of greatest population clustering occurred from 8000 to 5500 cal BP, which coincided with the rapid growth of populations identified in the Zahid et al. (2016) paper. Increasing dispersion of populations after 5500 cal BP coincides with the amelioration of environments after the Holocene thermal maximum (Shuman and Marsicek, 2016). It is also interesting that this pattern of increasing dispersion continues throughout the period of the mid-Holocene population plateau, as well as late Holocene population increases and declines (Fig. 3).

Fig. 4 shows the Clark-Evans *R* value as a function of the SPD. We interpret this figure as a measure of population clustering as a function of population size. This plot helps us further understand how spatial organization and population growth are directly related. At small population sizes, the *R* value indicates that the population is consistent with a random distribution. As populations began to grow, they were initially clustered, but after a brief period they continued to trend towards being dispersed across the landscape.

We interpret these results with the aid of models from population ecology. We derive a set of simple expectations for the *R* value as a function of population size (Fig. 6) for various ecological models (Fig. 5) to compare with Fig. 3.

4. Discussion: linking spatiotemporal analysis of radiocarbon data to population distribution models

4.1. Spatial analysis of radiocarbon SPDs

As mentioned above, we still lack an understanding of how different

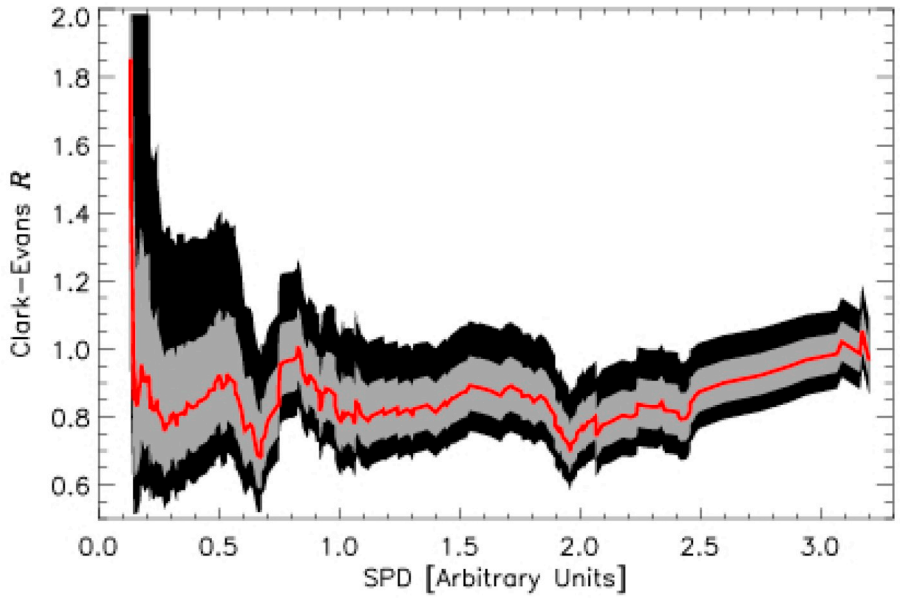

Fig. 4. Clark-Evans *R* as a function of the SPD. Red line is the mean *R* value of 10,000 realizations with grey and black representing the 68% and 95% confidence intervals, respectively. We boxcar smooth the data by 500 years. (For interpretation of the references to colour in this figure legend, the reader is referred to the Web version of this article.)

forms of social organization and mobility might impact radiocarbon date production. SPDs are often projected onto regions without considering either (a) the diachronic variability of land use within that region, or (b) the impacts of emigration or immigration between different regions.

Recent work has made progress using geospatial statistical techniques to better understand SPDs. Williams et al. (2013, 2015a, b) use k-means analysis to understand the diachronic variability in spatial clustering and to test hypotheses related to human colonization processes (Williams et al., 2015b), adaptive refugia (Williams et al., 2013), and the development of complex societies (Williams et al., 2015a) in Australia. Chaput et al. (2015) use kernel density analyses to understand the diachronic distribution of human populations across North America throughout the Holocene. Both of these methods focus on the second-order characteristics of spatial point processes and intensities (Bevan et al., 2013), which assume that clustering or cluster membership is already known. First-order analyses, on the other hand, seek to determine whether or not spatial clustering exists. Bevan et al. (2013, 31) note how "it is difficult, and often entirely misleading, to consider second-order effects without properly accounting for first-order effects". If SPDs are themselves first-order indicators of human population and occupation dynamics (Williams, 2012), then it might be productive to use simpler and less sophisticated spatial analyses that take first-order characteristics into account, before moving on to understanding cluster membership or spatial intensities.

The NNS (Clark and Evans, 1954) is one of the simplest tests available to determine spatial clustering of sites or populations. Conolly and Lake (2006, 164) note this prominence is due to it being "straightforward to calculate" and easy to interpret. They also point out its many limitations. For example, the greatest limitation of the NNS is its inability to compare beyond first nearest neighbors, which makes it ineffective for understanding multi-scalar processes (Bevan and Conolly, 2006; Conolly and Lake, 2006). However, despite its limitations, NNS is valuable for understanding general spatial dynamics, and is robust when used with Monte Carlo simulation (Bevan et al., 2013). While there are more sophisticated geospatial statistical tests available for understanding diachronic changes in radiocarbon SPDs, these analyses tend to be more difficult to interpret and they "fail to link theory and predictive models with spatial archaeological data" (Morgan, 2009, 389). We argue that NNS approaches to SPDs are valuable precisely because they are simple first-order approximations of more complex problems, making them easier to integrate with simple formal models from population ecology.

Without proper geographic considerations, human spatial distributions will always be clustered when measured by NNS. Physiography will always tend to cluster human land use patterns to some degree (e.g. humans prefer level terrain, and rarely focus habitations on mountain slopes or peaks), though we do not know what that baseline degree is. Wyoming is a region of mountains and basins, and as Fig. 1 shows, most of our dataset comes from basin regions. We argue that *R* values would be more biased if we had more upland occupations, as the natural clustering would obscure the role of settlement in these areas. Despite these natural limitations to NNS values, we argue that diachronic trends in *R* values should reflect real behavioral patterns, and these patterns should be structured by factors that can be modeled ecologically. We derive a set of expectations for the *R* values assuming the three different Ideal Distribution Models from population ecology.

4.2. Ideal Distribution Models

IDMs were developed in population ecology in order to understand habitat selection, specifically the relationship between habitat suitability and population density (Fretwell and Lucas, 1969). The models assume that habitat suitability varies in its ability to provide necessary resources for individuals, and therefore potential for sustaining certain animal populations. There are three variants of IDMs (Winterhalder and Kennett, 2006; Codding and Bird, 2015) which are differentiated by whether individuals are "free" to settle in their preferred habitat, and by negative versus positive density dependence of conspecifics (Fig. 5). Negative density dependence means that the addition of a new individual to a habitat diminishes the quality of the habitat, whereas positive density dependence means that the addition of a new individual enhances the quality of the habitat. Fig. 6 depicts each of the three IDM models described in Fig. 5 in terms of their expected NNI *R* values. The expected values are based on the difference between negative and positive density dependent expectations for the different IDM models, where *R* values > 1 are negative density dependent and values < are positive density dependent. We stress that these values are more relative than absolute measures of clustering or dispersion.

The population in an ideal free distribution (IFD) model has a negative density dependence (Fig. 5). Given two different habitats with different suitability, individuals are expected to inhabit the habitat with the highest suitability first. With the addition of each individual, the suitability of this habitat diminishes to a level where it is equal to the

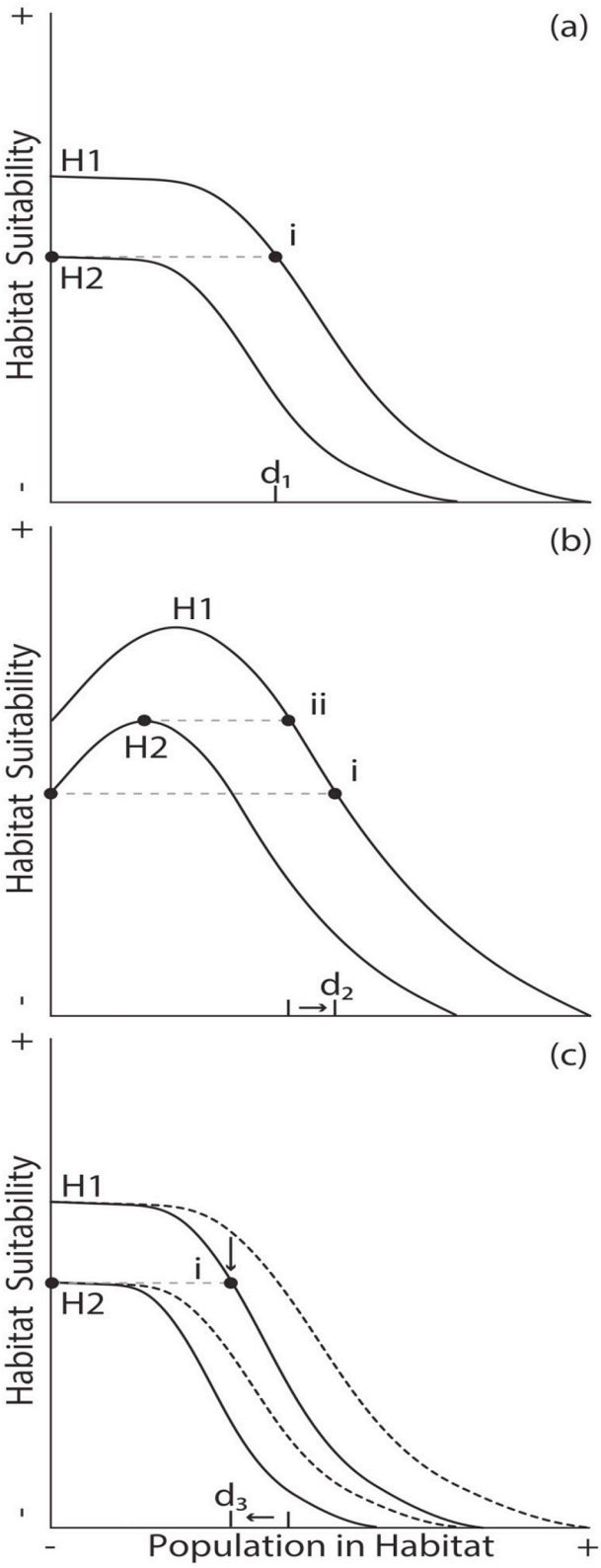

Fig. 5. Graphical representations of Ideal Distribution Models: a) ideal free distribution (IFD); b) ideal free distribution with Allee effects (IFDA); c) ideal despotic distribution (IDD) models. H1: Habitat 1; H2: Habitat 2. i and ii: suitability at which populations move to more suitable habitat. d_1, d_2, d_3: optimal population densities at which individuals should leave for a more suitable habitat. Two key things to notice: 1) Populations leave a habitat faster in ideal despotic distributions than in ideal free distributions; 2) In an Allee effect model, the increase of population leads to an increase of habitat suitability to a certain point, after which populations start to leave the habitat. From (Codding and Bird, 2015).

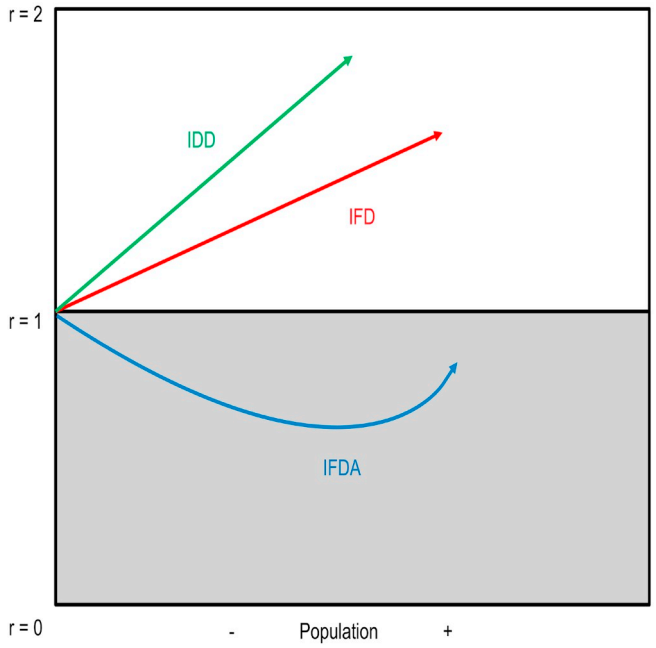

Fig. 6. Nearest neighbor values as population increases through time for the three different IDMs. IFD: red line; IDD: green line; IFDA: blue line. R > 1 represents dispersal of populations in space, and negative density dependence (white highlighted area); R < 1 represents clustering of populations in space, and positive density dependence (grey highlighted area). (For interpretation of the references to colour in this figure legend, the reader is referred to the Web version of this article.)

suitability of the second, lower ranking habitat. At this point, where the first and second habitats have equal productivity, individuals will then move to the second habitat. This process continues, with individuals eventually settling in habitats that were originally lower ranking. An IFD will yield a NNS of $R > 1$ (Fig. 6) due to its inherent negative density dependence. IFD models were the first IDMs to be applied to archaeological problems (Winterhalder and Kennett, 2006), and have also been the most widely applied in archaeology. Most applications of IFD models in archaeology have focused on the colonization of new landscapes (Kennett et al., 2006; McClure et al., 2006; Winterhalder and Kennett, 2006; Codding and Jones, 2013; Williams et al., 2015a; Jazwa et al., 2016). However, recent applications to complex societies (Jazwa and Jazwa, 2017; Prufer et al., 2017) illustrate their broader potential.

The second IDM adds positive density dependence to the IFD model. This model is referred to as the Ideal Free Distribution with Allee effects (IFDA) (Allee et al., 1949; Stephens et al., 1999; Greene and Stamps, 2001) (Fig. 5). The positive density dependence of IFDA means that as each individual is added to a habitat, the suitability of that habitat increases. Habitat suitability increases to a certain point, after which diminishing returns kick in, the habitat declines, and some individuals move to lesser quality habitats. IFDA models illustrate the power of populations working together to enhance the quality of their habitats, also known as increasing returns to scale. For this reason, IFDA models have been applied to research on transitions to agriculture (McClure et al., 2006). Recent work (Codding et al., 2017) has noted how larger cooperative groups display greater territorial behaviors. An IFDA will yield a NNS of $R < 1$ (Fig. 6) due to its positive density dependence, but over time a threshold is eventually passed in which groups start to bud off, leading to R values approaching 1, indicating increased dispersal of populations.

The Ideal Despotic Distribution (IDD) (Sutherland, 1996; Bell and Winterhalder, 2014) is negative density dependent like IFD (Fig. 5). However, the IDD is distinguished by the introduction of territorial

behavior. If individuals start actively defending high ranking habitats, then new individuals entering the region will be more quickly displaced to other lower ranking habitats. An IDD will yield a NNS of $R > 1$ (Fig. 6). Because of territorial exclusion in an IDD system, populations will disperse at faster rates than IFD models, which means that R values will increase more rapidly than in an IFD system. Discriminating between an IDD and IFD is possible with additional archaeological information, i.e., evidence of defensive architecture and violence (Jazwa et al., 2017; Prufer et al., 2017). The role of territoriality in IDD models has enabled them to be useful in considering the tempo and processes of demographic expansion (Shennan, 2007; Kennett and Winterhalder, 2008) and the dynamics of complex societies (Williams et al., 2015a; Prufer et al., 2017; Jazwa et al., 2017).

We propose that each of the different IDM variants will produce different temporal structure in the spatial distribution of populations. Recent work applying IDMs to archaeological problems have focused on oscillations between different kinds of IDMs (McClure et al., 2006; Williams et al., 2015a; Prufer et al., 2017). McClure et al. (2006) focus on the transition between an IFD and an IFDA during the Neolithic period in Spain. Williams et al. (2015a) and Prufer et al. (2017) focus on transitions between IFD and IDD systems in the development and transitions of complex societies in Australia and Mesoamerica. One of the remaining challenges is understanding the relationships between IFDA and IDD systems. In other words, an understanding of the circumstances under which cooperative or competitive behavior is the dominant social dynamic.

The central challenge in discriminating between IDD and IFDA models as populations increase over time is that these systems can start to reveal similar qualities (Bell and Winterhalder, 2014). As, for example, when IDD models flip to positive density dependent situations due to despots providing certain concessions to keep people in their territories in order to take advantage of their labor (Bell and Winterhalder, 2014). However, because this example of an IDD flipping to a positive density dependent situation is controlled by a despot within a firm social-political structure, we expect there to be an abrupt shift from high R values to low R values that will be easily revealed in time-series patterns. Patterns for an IFDA will change less abruptly, and will not be as heavily clustered as those from an IDD. Nevertheless, because both IDD and IFDA can be dynamic as population grows through time, we still expect an IFDA to possibly move from a more clustered to a more dispersed pattern as positive density dependence approaches local or regional carrying capacities. As with the comparisons of IDD to IFD, in IFDA situations, R values will not cluster or disperse as abruptly as we would expect from IDD situations with despots having firm control over rates of clustering or dispersal. Furthermore, as mentioned above, these different models can be delineated by the analysis of other archaeological proxies.

4.3. Applying IDMs to SPDs in space

We seek to understand whether rates of population growth from 12000 to 6000 cal BP reflect an IFD in which regional carrying capacities are yet to be reached (Bettinger, 2016) and, in particular, if spatial distributions of populations in Wyoming during the period of population stasis from 6000 to 4500 cal BP, and population decline from 4500 to 2000 cal BP, reflects different spatial distributions indicative of other IDM models. The NNS trends in Fig. 3B reveal that the period of population stasis occurs during a transition from a relatively clustered to an increasingly dispersed population. The period of population decline occurs during this continued period of dispersed populations. These results suggest that population growth, stasis and decline have correspondent oscillations in spatial distributions of prehistoric populations. Importantly, these trends highlight that population growth from 12000 to 6000 cal BP did not occur during a period in which populations could increasingly bud off from each other and inhabit other regions in a negative density dependent IFD situation, but rather, that population growth occurred during relatively clustered social organizations in a positive density dependent Allee-like situation. The population decline after 4500 cal BP also corresponds with ecological theory that eventually Allee effects have negative impacts on population growth, as they make populations vulnerable to disease transmission and local and global extinction over time (Stephens and Sutherland, 1999).

SPD approaches require the use of multiple proxies, in the forms of other lines of archaeological evidence (Williams, 2012; Crombé and Robinson, 2014), in order to move from first-order pattern recognition of population trajectories to an understanding of human behavioral change. The same is true for testing hypotheses for different IDMs for particular periods of time.

The Wyoming case study provides evidence to corroborate the interpretation of Allee effects leading to early-mid Holocene population growth and stasis. The period of greatest population growth and relative settlement clustering in Wyoming, from ca. 8000-5500 cal BP, corresponds with the appearance and proliferation of pithouse architecture. This period comprises around 70% of the total pithouses excavated during the Archaic period in Wyoming (Buenger and Goodrick, 2017). Pithouses decrease dramatically after ca. 5000 cal BP (Buenger and Goodrick, 2017), during which time there is stasis in population growth and increasing dispersal of populations. Pithouse architecture has been interpreted as seasonal occupations that were used persistently from one season to the next by small family groups who would focus on predictable plant and animal resources (Smith, 2003; Smith and McNees, 2011; Buenger and Goodrick, 2017). Use of spatial organization in this way would enable groups to pool their labor for more efficient extraction of resources (Smith and McNees, 2011). This pooling of labor generated increasing returns and enhanced the suitability of habitats, which as highlighted above, are hallmarks of Allee effects. The relative spatial clustering of populations during this time is indicative of within-group cooperation driven by Allee effects associated with intensive economies (Codding et al., 2017), in this case predictable plant and animal resources during spring and fall, which were the leanest time of the year in Wyoming (Smith, 2003). As mentioned above, this period of greatest relative population clustering also corresponds to the end of the Holocene thermal maximum (Shuman and Marsicek, 2016), during which it would have been even more challenging to capture resources, and likely provided even greater motivations for pooling labor resources. However, eventually, the negative impacts of Allee effects started to kick in, as evidenced by the decline of pithouses, the increasing dispersal of populations, and the overall decline of population sizes.

Much work remains to further test the possible negative impacts of Allee effects on the sustainability of populations and the possible roles of disease transmission and other social or ecological processes. For the time being, our aim in this paper has been to introduce an integrated theory and method that can begin to provide testable hypotheses that will be the subject of future research.

5. Conclusion

We develop a simple method for mapping radiocarbon SPDs in space that is explicitly integrated with a theoretical framework from population ecology. Future work to better understand higher-order properties of the spatial distribution of radiocarbon time series will employ more sophisticated statistical techniques.

One of the outstanding challenges in using large radiocarbon date time series (SPDs) to understand population growth throughout prehistory concerns the possibility that inflections in time series are indicative of changes in social organizational processes. In this paper we have employed a simple first-order spatial statistic allowing us to compare with different models from population ecology. Our results suggest that prehistoric population growth throughout the Holocene in Wyoming occurred during relatively more clustered and cooperative,

positive density dependent situations. By developing methods of spatiotemporal analysis, we can begin to understand how radiocarbon time series reflect important prehistoric shifts to territoriality and competition within/between societies, as well as when societies transition to cooperative and positive density dependent economies of scale.

Data release statement

The radiocarbon dates used for the analysis can be found in the Canadian Archaeological Radiocarbon Database (http://www.canadianarchaeology.ca). The analyses in this paper rely on precise locational data of archaeological sites. Unfortunately, publishing or making such data publically available is a potentially criminal offense under Section 9 of the Archaeological Resources Protection Act of 1979. In addition, publishing precise locational data would violate the Society for American Archaeology's Ethical Principle 1: “It is the responsibility of all archaeologists to work for the long-term conservation and protection of the archaeological record by practicing and promoting stewardship of the archaeological record,” and Ethical Principle 6: “An interest in preserving and protecting in situ archaeological sites must be taken in to account when publishing and distributing information about their nature and location.” We can share our data with researchers who are vetted through the appropriate state authorities.

See Zellmer, L.R. 2017. Protected Places: A Survey of Laws on Archaeological Site and Cave Location Confidentiality and Their Potential Impact on Library Reference Policies and Services. J. Map and Geography Libraries 13 (2): 148–174.

Acknowledgements

We thank the Wyoming State Historic Preservation Office for making data available. We thank Nick Holmes for helpful discussion regarding the spatial analysis. We gratefully acknowledge financial support provided by National Science Foundation grants BCS 14-18858 and 16-24061 (to RLK and ER). HJZ is supported by the Clay Postdoctoral Fellowship.

References

Allee, W.C., Park, O., Emerson, A.E., Park, T., Schmidt, K.P., et al., 1949. Principles of Animal Ecology. WB Saunders, Philadelphia Technical Report.
Armit, I., Swindles, G.T., Becker, K., 2013. From dates to demography in later prehistoric Ireland? experimental approaches to the meta-analysis of large 14c data-sets. J. Archaeol. Sci. 40, 433–438.
Bamforth, D.B., Grund, B., 2012. Radiocarbon calibration curves, summed probability distributions, and early paleoindian population trends in North America. J. Archaeol. Sci. 39, 1768–1774.
Bell, A.V., Winterhalder, B., 2014. The population ecology of despotism. Hum. Nat. 25, 121–135.
Bettinger, R.L., 2016. Prehistoric hunter–gatherer population growth rates rival those of agriculturalists. Proc. Natl. Acad. Sci. Unit. States Am. 113, 812–814.
Bevan, A., Conolly, J., 2006. Multiscalar approaches to settlement pattern analysis. In: Confronting Scale in Archaeology. Springer, pp. 217–234.
Bevan, A., Crema, E., Li, X., Palmisano, A., 2013. Intensities, interactions, and uncertainties: some new approaches to archaeological distributions. In: Bevan, A., Lake, M. (Eds.), Computational Approaches to Archaeological Spaces. Left Coast Press Walnut Creek, pp. 27–52.
Bluhm, L.E., Surovell, T.A., 2018. Validation of a global model of taphonomic bias using geologic radiocarbon ages. Quat. Res. 1–4.
Brown, W.A., 2015. Through a filter, darkly: population size estimation, systematic error, and random error in radiocarbon-supported demographic temporal frequency analysis. J. Archaeol. Sci. 53, 133–147.
Buenger, B.A., Goodrick, S.R., 2017. Mid-holocene hunter-gatherers, housepits, and landscape reuse: sweetwater river, Wyoming. Plains Anthropol. 1–22.
Carleton, W.C., Campbell, D., Collard, M., 2018. Radiocarbon dating uncertainty and the reliability of the pewma method of time-series analysis for research on long-term human-environment interaction. PloS One 13, e0191055.
Chaput, M.A., Gajewski, K., 2016. Radiocarbon dates as estimates of ancient human population size. Anthropocene 15, 3–12.
Chaput, M.A., Kriesche, B., Betts, M., Martindale, A., Kulik, R., Schmidt, V., Gajewski, K., 2015. Spatiotemporal distribution of holocene populations in North America. Proc. Natl. Acad. Sci. Unit. States Am. 112, 12127–12132.
Clark, P.J., Evans, F.C., 1954. Distance to nearest neighbor as a measure of spatial relationships in populations. Ecology 35, 445–453.
Codding, B.F., Bird, D.W., 2015. Behavioral ecology and the future of archaeological science. J. Archaeol. Sci. 56, 9–20.
Codding, B.F., Jones, T.L., 2013. Environmental productivity predicts migration, demographic, and linguistic patterns in prehistoric California. Proc. Natl. Acad. Sci. Unit. States Am. 110, 14569–14573.
Codding, B.F., Parker, A.K., Jones, T.L., 2017. Territorial behavior among Western North American foragers: allee effects, within group cooperation, and between group conflict. Quat. Int. https://doi.org/10.1016/j.quaint.2017.10.045.
Conolly, J., Lake, M., 2006. Geographical Information Systems in Archaeology. Cambridge University Press.
Contreras, D.A., Meadows, J., 2014. Summed radiocarbon calibrations as a population proxy: a critical evaluation using a realistic simulation approach. J. Archaeol. Sci. 52, 591–608.
Crema, E., Bevan, A., Shennan, S., 2017. Spatio-temporal approaches to archaeological radiocarbon dates. J. Archaeol. Sci. 87, 1–9.
Crema, E.R., Bevan, A., Lake, M.W., 2010. A probabilistic framework for assessing spatio-temporal point patterns in the archaeological record. J. Archaeol. Sci. 37, 1118–1130.
Crema, E.R., Habu, J., Kobayashi, K., Madella, M., 2016. Summed probability distribution of 14c dates suggests regional divergences in the population dynamics of the Jomon period in Eastern Japan. PloS One 11, e0154809.
Crombé, P., Robinson, E., 2014. 14c dates as demographic proxies in neolithisation models of Northwestern Europe: a critical assessment using Belgium and Northeast France as a case-study. J. Archaeol. Sci. 52, 558–566.
Downey, S.S., Bocaege, E., Kerig, T., Edinborough, K., Shennan, S., 2014. The neolithic demographic transition in Europe: correlation with juvenility index supports interpretation of the summed calibrated radiocarbon date probability distribution (scdpd) as a valid demographic proxy. PloS One 9, e105730.
Freeman, J., Byers, D.A., Robinson, E., Kelly, R.L., 2018. Culture process and the interpretation of radiocarbon data. Radiocarbon 60, 453–467.
Fretwell, S.D., Lucas, H.L., 1969. On territorial behavior and other factors influencing habitat distribution in birds. Acta Biotheor. 19, 16–36.
Goldberg, A., Mychajliw, A.M., Hadly, E.A., 2016. Post-invasion demography of prehistoric humans in South America. Nature 532, 232.
Greene, C.M., Stamps, J.A., 2001. Habitat selection at low population densities. Ecology 82, 2091–2100.
Jazwa, C.S., Jazwa, K.A., 2017. Settlement ecology in bronze age messenia. J. Anthropol. Archaeol. 45, 157–169.
Jazwa, C.S., Kennett, D.J., Winterhalder, B., 2016. A test of ideal free distribution predictions using targeted survey and excavation on California's Northern channel Islands. J. Archaeol. Method Theor 23, 1242–1284.
Jazwa, C.S., Kennett, D.J., Winterhalder, B., Joslin, T.L., 2017. Territioriality and the rise of despotic social organization on Western Santa Rosa Island, California. Quat. Int. https://doi.org/10.1016/j.quaint.2017.11.009.
Kelly, R.L., Surovell, T.A., Shuman, B.N., Smith, G.M., 2013. A continuous climatic impact on holocene human population in the rocky mountains. Proc. Natl. Acad. Sci. Unit. States Am. 110, 443–447.
Kennett, D.J., Anderson, A., Winterhalder, B., et al., 2006. The ideal free distribution, food production, and the colonization of oceania. In: Behavioral Ecology and the Transition to Agriculture. University of California Press, pp. 265–288.
Kennett, D.J., Winterhalder, B., 2008. Demographic expansion, despotism and the colonisation of East and South Polynesia. In: Islands of Inquiry: Colonisation, Seafaring and the Archaeology of Maritime Landscapes (Terra Australis 29). Australia National University Press, Canberra, pp. 87–96.
McClure, S.B., Jochim, M.A., Barton, C.M., 2006. Human behavioral ecology, domestic animals, and land use during the transition to agriculture in Valencia, Eastern Spain. In: Behavioral Ecology and the Transition to Agriculture, pp. 197–216.
Morgan, C., 2009. Climate change, uncertainty and prehistoric hunter–gatherer mobility. J. Anthropol. Archaeol. 28, 382–396.
Naudinot, N., Tomasso, A., Tozzi, C., Peresani, M., 2014. Changes in mobility patterns as a factor of 14c date density variation in the late epigravettian of Northern Italy and Southeastern France. J. Archaeol. Sci. 52, 578–590.
Onkamo, P., Kammonen, J., Pesonen, P., Sundell, T., Moltchanova, E., Oinonen, M., Haimila, M., Arjas, E., 2012. Bayesian spatiotemporal analysis of radiocarbon dates from Eastern Fennoscandia. Radiocarbon 54, 649–659.
Park, J., Wright, D.K., Kim, J., 2017. Change in settlement distribution and the emergence of an early state: a spatial analysis of radiocarbon dates from Southwestern Korea. Radiocarbon 59, 1779–1791.
Perez, S.I., Postillone, M.B., Rindel, D., Gobbo, D., Gonzalez, P.N., Bernal, V., 2016. Peopling time, spatial occupation and demography of late pleistocene–holocene human population from patagonia. Quat. Int. 425, 214–223.
Peros, M.C., Munoz, S.E., Gajewski, K., Viau, A.E., 2010. Prehistoric demography of North America inferred from radiocarbon data. J. Archaeol. Sci. 37, 656–664.
Perry, G.L., Miller, B.P., Enright, N.J., 2006. A comparison of methods for the statistical analysis of spatial point patterns in plant ecology. Plant Ecol. 187, 59–82.
Prufer, K.M., Thompson, A.E., Meredith, C.R., Culleton, B.J., Jordan, J.M., Ebert, C.E., Winterhalder, B., Kennett, D.J., 2017. The classic period maya transition from an ideal free to an ideal despotic settlement system at the polity of Uxbenká. J. Anthropol. Archaeol. 45, 53–68.
Reimer, P.J., Bard, E., Bayliss, A., Beck, J.W., Blackwell, P.G., Ramsey, C.B., Buck, C.E., Cheng, H., Edwards, R.L., Friedrich, M., et al., 2013. Intcal13 and marine13 radiocarbon age calibration curves 0–50,000 years cal bp. Radiocarbon 55, 1869–1887.
Rhode, D., Brantingham, P.J., Perreault, C., Madsen, D.B., 2014. Mind the gaps: testing for hiatuses in regional radiocarbon date sequences. J. Archaeol. Sci. 52, 567–577.
Rick, J.W., 1987. Dates as data: an examination of the Peruvian preceramic radiocarbon record. Am. Antiq. 52, 55–73.

Shennan, S., 2007. The spread of farming into central Europe and its consequences: evolutionary models. In: The Model-Based Archaeology of Socionatural Systems, pp. 141–156.
Shennan, S., Downey, S.S., Timpson, A., Edinborough, K., Colledge, S., Kerig, T., Manning, K., Thomas, M.G., 2013. Regional population collapse followed initial agriculture booms in mid-holocene Europe. Nat. Commun. 4, 2486.
Shennan, S., Edinborough, K., 2007. Prehistoric population history: from the late glacial to the late neolithic in central and Northern Europe. J. Archaeol. Sci. 34, 1339–1345.
Shuman, B.N., Marsicek, J., 2016. The structure of holocene climate change in mid-latitude North America. Quat. Sci. Rev. 141, 38–51.
Smith, C.S., 2003. Hunter–gatherer mobility, storage, and houses in a marginal environment: an example from the mid-holocene of Wyoming. J. Anthropol. Archaeol. 22, 162–189.
Smith, C.S., McNees, L.M., 2011. Persistent land use patterns and the mid-holocene housepits of Wyoming. J. Field Archaeol. 36, 298–311.
Stephens, P.A., Sutherland, W.J., 1999. Consequences of the allee effect for behaviour, ecology and conservation. Trends Ecol. Evol. 14, 401–405.
Stephens, P.A., Sutherland, W.J., Freckleton, R.P., 1999. What is the allee effect? Oikos 185–190.
Surovell, T.A., Brantingham, P.J., 2007. A note on the use of temporal frequency distributions in studies of prehistoric demography. J. Archaeol. Sci. 34, 1868–1877.
Surovell, T.A., Finley, J.B., Smith, G.M., Brantingham, P.J., Kelly, R., 2009. Correcting temporal frequency distributions for taphonomic bias. J. Archaeol. Sci. 36, 1715–1724.
Sutherland, W.J., 1996. From Individual Behaviour to Population Ecology, vol. 11 Oxford University Press on Demand.
Tallavaara, M., Luoto, M., Korhonen, N., Järvinen, H., Seppä, H., 2015. Human population dynamics in Europe over the last glacial maximum. Proc. Natl. Acad. Sci. Unit. States Am. 112, 8232–8237.
Timpson, A., Colledge, S., Crema, E., Edinborough, K., Kerig, T., Manning, K., Thomas, M.G., Shennan, S., 2014. Reconstructing regional population fluctuations in the European neolithic using radiocarbon dates: a new case-study using an improved method. J. Archaeol. Sci. 52, 549–557.
Torfing, T., 2015. Neolithic population and summed probability distribution of 14c-dates. J. Archaeol. Sci. 63, 193–198.
Velázquez, E., Martínez, I., Getzin, S., Moloney, K.A., Wiegand, T., 2016. An evaluation of the state of spatial point pattern analysis in ecology. Ecography 39, 1042–1055.
Wang, C., Lu, H., Zhang, J., Gu, Z., He, K., 2014. Prehistoric demographic fluctuations in China inferred from radiocarbon data and their linkage with climate change over the past 50,000 years. Quat. Sci. Rev. 98, 45–59.
Williams, A.N., 2012. The use of summed radiocarbon probability distributions in archaeology: a review of methods. J. Archaeol. Sci. 39, 578–589.
Williams, A.N., Ulm, S., Cook, A.R., Langley, M.C., Collard, M., 2013. Human refugia in Australia during the last glacial maximum and terminal pleistocene: a geospatial analysis of the 25–12 ka Australian archaeological record. J. Archaeol. Sci. 40, 4612–4625.
Williams, A.N., Ulm, S., Turney, C.S., Rohde, D., White, G., 2015a. Holocene demographic changes and the emergence of complex societies in prehistoric Australia. PloS One 10, e0128661.
Williams, A.N., Veth, P., Steffen, W., Ulm, S., Turney, C.S., Reeves, J.M., Phipps, S.J., Smith, M., 2015b. A continental narrative: human settlement patterns and Australian climate change over the last 35,000 years. Quat. Sci. Rev. 123, 91–112.
Winterhalder, B., Kennett, D.J., 2006. Behavioral ecology and the transition from hunting and gathering to agriculture. In: Behavioral Ecology and the Transition to Agriculture. 1–21.
Zahid, H.J., Robinson, E., Kelly, R.L., 2016. Agriculture, population growth, and statistical analysis of the radiocarbon record. Proc. Natl. Acad. Sci. Unit. States Am. 113, 931–935.